INFECTION AND IMMUNITY, Oct. 2009, p. 4362–4370 Vol. 77, No. 10
0019-9567/09/$08.00+0 doi:10.1128/IAI.00044-09

Characterization of a Unique ADP-Ribosyltransferase of *Mycoplasma penetrans*▽

Coreen Johnson, T. R. Kannan, and Joel B. Baseman*

Department of Microbiology and Immunology, University of Texas Health Science Center at San Antonio, 7703 Floyd Curl Drive, MC 7758, San Antonio, Texas 78229-3900

Received 13 January 2009/Returned for modification 22 February 2009/Accepted 25 July 2009

Mycoplasma penetrans **is a urogenital tract pathogen implicated in the deterioration of the immune system in human immunodeficiency virus-infected AIDS patients. Here, we describe a 78-kDa protein from *M. penetrans*, designated MYPE9110, that exhibits sequence similarity to known ADP-ribosyltransferases (ADPRTs) such as *Bordetella pertussis* pertussis toxin and *Mycoplasma pneumoniae* community-acquired respiratory distress syndrome toxin. MYPE9110 possesses key amino acid residues found in all ADPRTs that are essential for ADPRT activity. Several mammalian cell proteins are ADP-ribosylated by MYPE9110, and the full-length recombinant protein exhibits a strong auto-ADP-ribosylating activity. In the absence of target proteins, MYPE9110 demonstrates a NAD-glycohydrolase activity by hydrolyzing NAD. Furthermore, this toxin elicits cytopathology in HeLa cells by inducing cytoplasmic vacuolization in the presence of ammonium chloride. The deletion of the C-terminal region of MYPE9110 significantly diminishes its binding to host cells while still exhibiting an ADPRT activity, suggesting that MYPE9110 is a member of the family of A-B ADPRT toxins.**

The *Mollicutes* contain several human-pathogenic mycoplasmas including *Mycoplasma pneumoniae*, *Mycoplasma genitalium*, and *Mycoplasma penetrans*. *M. penetrans* GTU-54 was first isolated from the urine of a human immunodeficiency virus (HIV)-positive homosexual male (20). Subsequent studies reported a higher frequency of antibodies against *M. penetrans* (40%) in sera of HIV-infected AIDS patients than in sera of HIV-infected non-AIDS and HIV-negative control groups (20% and 0.3%, respectively) (36). It was previously hypothesized that *M. penetrans* could exist as either an opportunist or a cofactor in AIDS progression for several reasons, including the ability of *M. penetrans* to activate human T lymphocytes (31). Although considered predominately a urogenital tract pathogen, *M. penetrans* strains have also been isolated from blood (strain HF-1) and respiratory tract cultures (strain HF-2) of a non-HIV-infected patient with primary antiphospholipid syndrome and bacteremia (37).

Among the genome-sequenced pathogenic mycoplasmas, *M. penetrans* strain HF-2 is the largest, at 1.4 Mbp, with a low G+C content of 25.7% and 1,038 predicted coding sequences (32). The genome consists of many paralogs, including the *p35* gene family, which may account for its larger genome size than other pathogenic mycoplasmas. The *p35* gene family encodes surface lipoproteins, including the immunodominant P35 protein, which is the basis of the serological diagnosis of *M. penetrans* infection (32). In silico analysis of the *M. penetrans* genome indicates the presence of a two-component response regulator (MYPE3960) and a putative sensory transduction histidine kinase (MYPE2360). No such regulatory elements have been found for other sequenced mollicute genomes, suggesting that *M. penetrans* is unique in that it may be able to sense and synthesize proteins in response to its survival niche (32).

Following adherence to host cells, *M. penetrans* induces cytoskeleton rearrangement, as evidenced by the aggregation of tubulin and α-actinin (13). This event leads to the internalization of *M. penetrans*, where it resides in the host cell cytosol, membrane-bound vacuoles, or perinuclear region for extended periods of time (2, 10, 13). This intracellular environment offers many benefits to the bacterium, where it can avoid host immune responses and acquire essential nutrients (26). The mechanism by which *M. penetrans* triggers cytoskeletal rearrangements is still poorly understood. Manipulation of the cytoskeletal network by bacterial toxins, including ADP-ribosylating toxins, was previously reported for both gram-negative and gram-positive bacteria (26). Until recently, the only genome-encoded potential virulence factors of *M. penetrans* included endonucleases, hemolysins, and proteases (3, 18, 32), and their roles in pathogenesis remain unclear.

Recently, an ADP-ribosylating and vacuolating toxin was described for *M. pneumoniae* (17). This toxin, designated community-acquired respiratory distress syndrome (CARDS) toxin, was first identified by its interaction with the human lung protein surfactant protein A and by its limited but critically relevant sequence similarity to the *Bordetella pertussis* pertussis toxin S1 subunit ADP-ribosyltransferase (ADPRT) domain (17, 19). ADPRTs are found in a wide range of bacterial pathogens and catalyze the transfer of a single ADP-ribosyl group from β-NAD onto specific amino acid residues of host cell proteins with the release of nicotinamide (24). Mono-ADP-ribosylation by these ADPRTs leads to the modification of various host cell target proteins and their activities, including the inhibition of host protein synthesis by diphtheria toxin (DT) (25), alterations in signal transduction pathways by pertussis toxin (21), and interference of actin polymerization by *Clostridium* iota and C2 toxins (1, 33). Many members of these

* Corresponding author. Mailing address: Department of Microbiology and Immunology, University of Texas Health Science Center at San Antonio, 7703 Floyd Curl Drive, MC 7758, San Antonio, TX 78229-3900. Phone: (210) 567-3939. Fax: (210) 567-6491. E-mail: baseman@uthsca.edu.

▽ Published ahead of print on 3 August 2009.

TABLE 1. Primers used for amplification and site-directed mutagenesis of the MYPE9110 gene

Primer	Sequence[a]	Annealing temp (°C)	Positions
MYPE9110 FP	5′-**CATATG**ATTAACAATTGATATTAAATCATCTTGG-3′	54	1→30
MYPE9110 RP	5′-**GGATCC**TTACTTAATATGATTTTCATTAAG-3′	53	1921←1944
MYPE9110 F2	5′-GACAAAATATCTTCATGGATGAATGTTC-3′	54	724→751
MYPE9110 R2	5′-GAACATTCATCCATGAAGATATTTTGTC-3′	54	724←751
MYPE9110 R2.5	5′-GATATTTTGATAAATTAACTTTCTGCCATTC-3′	54	1742←1711
MYPE9110 F3	5′-CATTAATTTATCATGGATGTGGAAATATC-3′	53	1458→1486
MYPE9110 F3.5	5′-GATGGGAAACCATATAGATGGTTAGAATGGCAG-3′	62	1687→1719
MYPE9110 R3.5	5′-CTTTGTCATATCTACATTTTTTCAAAACCCACATAT TATTTTTATTTGG-3′	61	1741←1775
MYPE9110 R3	5′-GATATTTCCACATCCATGATAAATTAATG-3′	53	1458←1486
MYPE9110 F4.5	5′-CCAAATAAAAATAATATGTGGGTTTTG-3′	51	1741→1767
MYPE9110 R4.5	5′-GCACCCATAAATAACCATTATTG-3′	50	1714←1740
MYPE9110 F5.5	5′-GATTATCAGTTTTTTCAATAATGGTTATTTATG-3′	53	1801→1826

[a] In the given primer sequences, TGA-to-TGG changes are underlined, and the introduced restriction endonuclease sites are in boldface type.

ADPRTs, including pertussis toxin and DT, belong to the A-B family, which possesses an active ADPRT subunit, known as the A subunit, and a B subunit responsible for the binding and translocation of the active subunit across host cell membranes (11).

Our discovery of CARDS toxin in *M. pneumoniae* prompted us to look at other mycoplasma genomes for the existence of a related protein. A hypothetical protein in the *M. penetrans* genome, annotated MYPE9110, shared sequence similarity with CARDS toxin and a conserved domain with the pertussis toxin S1 subunit. In this study we show that MYPE9110 is related to the family of classical A-B toxins, as it possesses an N-terminal ADPRT domain and a C-terminal cell-binding domain. We also show that MYPE9110 elicits cytopathology in host cells, indicating the virulence potential of this newly characterized *M. penetrans* protein.

MATERIALS AND METHODS

Bacterial cultures and growth conditions. *Mycoplasma penetrans* GTU-54 is a clinical isolate kindly provided by Shyh-Ching Lo (Armed Forces Institute of Pathology, Washington, DC) (20). Clinical isolates from Texas and France were obtained from J. G. Tully (National Institute of Allergy and Infectious Diseases, Bethesda, MD). These isolates were routinely grown at 37°C overnight in SP-4 broth with no aeration in 150-cm^2 tissue culture flasks. *Escherichia coli* BL21(DE3) *lpxM* was used to express recombinant MYPE9110 and was kindly provided by Jean-Francois Gauchat (7).

Eukaryotic cell growth conditions. HeLa cells (ATCC CCL-2) were obtained from the American Type Culture Collection (ATCC) and passaged in minimal essential medium (MEM) (ATCC) with 10% fetal bovine serum (FBS) (Atlas Biologicals). Cells were grown at 37°C in 5% CO_2 in 75-cm^2 flasks.

Transcriptional analysis. *M. penetrans* GTU-54 cultures were grown in SP-4 broth at 37°C, and cells were harvested at 3-, 6-, 12-, 18-, 24-, and 30-h growth intervals, washed, and suspended in phosphate-buffered saline (PBS) (pH 7.4). Cell turbidity was measured at an optical density at 600 nm to study growth patterns. Reverse transcription (RT)-PCR was performed using 5 μg total RNA extracted at each time point with Tri reagent (Sigma). RNA was incubated in the presence or absence of reverse transcriptase (Superscript II reverse transcriptase; Invitrogen) and MYPE9110 or *tufA* gene-specific primers in order to generate cDNA and ascertain DNA contamination, respectively. PCR amplification of *M. penetrans* MYPE9110 (n = 30 cycles) was performed with the following primers, corresponding to the internal region, nucleotides 724 to 1119, of MYPE9110: MYPE9110-FP2 (5′-GACAAAATATCTTCATGGATGAATGTTC-3′) and reverse primer MYPE9110RT-RP (5′-GAAGTCAAAAATAAATCTACCTGATTTATC-3′). PCR amplification of the *M. penetrans tufA* gene (MYPE320) was performed with primers corresponding to the internal region of nucleotides 505 to 906 of *tufA* by using EF-Tu FP (5′-ATGGCAAAACAAAGTTTGATAGATCAAAAG-3′) and EF-Tu RP (5′-TTATCTAATAACTTTAGTTACTGTACCAGC-3′). To determine whether MYPE9110 was secreted during *M. penetrans* growth, supernatants of exponentially grown cultures were ammonium sulfate precipitated (30, 50, and 80% saturations). Each fraction was desalted, concentrated, and separated on sodium dodecyl sulfate (SDS)-polyacrylamide gels. Analysis was performed by Western blotting with polyclonal rabbit antibody generated against MYPE9110.

Construction of rMYPE9110 and its derivative plasmids. *M. penetrans* GTU-54 genomic DNA (Easy DNA kit; Invitrogen) served as a template to amplify MYPE9110 by PCR using MYPE9110-specific oligonucleotide primers. The construction and TGA corrections of full-length MYPE9110 were accomplished with primers listed in Table 1. Overlap extension PCR (14) was used to generate the full-length MYPE9110 gene product, which involved the overlap and annealing of six individual DNA fragments amplified with *Pfu* Turbo DNA polymerase (Stratagene) and mutagenic primers (Table 1). The MYPE9110 PCR product was amplified with Platinum *Taq* polymerase (Invitrogen), cloned in the TOPO pCRII-TA cloning vector (Invitrogen), transformed into *Escherichia coli* Top10 cells (Invitrogen), digested with NdeI and BamHI endonucleases (New England Biolabs), and ligated (T4 DNA ligase; New England Biolabs) with expression vector pET-19b (EMD Biosciences), which had been treated with the same enzymes. *E. coli* Top10 cells were transformed with the ligated mixture, and several transformants were isolated. The selection of recombinant MYPE9110 (rMYPE9110) transformants was accomplished by restriction digestion with NdeI and BamHI endonucleases and by sequencing of positive clones. Similarly, using primers presented in Table 2, rMYPE9110 N-terminal (rN-MYPE9110$^{1\text{-}300}$), C-terminal (rC-MYPE9110$^{302\text{-}647}$), rMYPE9110$^{156\text{-}Glu\text{-}Ala}$, and rMYPE9110$^{156\text{-}Glu\text{-}Asp}$ constructs were amplified and cloned in the same manner as that described above. Sequencing of all constructs was performed in the Department of Microbiology and Immunology Nucleic Acids Facility (University of Texas Health Science Center at San Antonio). Sequences were analyzed using the Basic Local Alignment Sequence Tool (BLAST) program available from the NCBI database.

Expression and purification of rMYPE9110 and its derivatives. *E. coli* BL21(DE3) *lpxM* was transformed with plasmid pET-MYPE9110 and grown in standard Luria-Bertani broth (LB) containing 100 μg ml^{-1} ampicillin (Sigma) at 37°C with aeration. To increase the yield of soluble protein, cultures were grown at 30°C to an optical density at 600 nm of 0.4 and induced with 200 μM IPTG (isopropyl-β-D-thiogalactopyranoside) (Sigma) at 30°C for 5 h with aeration (200 rpm). Recombinant His_{10}-tagged MYPE9110 (rMYPE9110) was purified from *E. coli* BL21(DE3) *lpxM* cells under native conditions by nickel affinity chromatography according to the manufacturer's protein isolation protocol (Qiagen), with slight modifications. Briefly, cells were lysed by sonication and collected by centrifugation at 10,000 × *g* for 30 min at 4°C. rMYPE9110 was bound to the nickel affinity column, eluted, desalted in 50 mM Tris with 5% glycerol (pH 7.4) using PD-10 columns (GE Healthcare), concentrated by filtration (Amicon) according to the manufacturer's instructions (Millipore), quantified with bicinchoninic acid (Pierce), and stored at −80°C. rMYPE9110 was sequenced by matrix-assisted laser desorption ionization–time of flight analysis at the microsequencing facility at Baylor College of Medicine (Houston, TX). The rN-MYPE9110$^{1\text{-}300}$, rC-MYPE9110$^{302\text{-}647}$, rMYPE9110$^{Glu\text{-}Ala}$, and rMYPE9110$^{Glu\text{-}Asp}$ proteins were also expressed as His-tagged recombinant proteins and purified under the same conditions as those described above for full-length wild-type MYPE9110. However, expression of the C-terminal and active-site mutant proteins did not yield sufficient levels of soluble proteins.

TABLE 2. Primers used for generating truncated and catalytic-site-modified proteins

Primer for truncation/mutagenesis of MYPE9110	Sequence[a]
N-terminal FP (MYPE9110 FP)	5′-**CATATG**ATTAACAATTGATATTAAATCATCTTGG-3′
N-terminal RP	5′-**GGATCC**CTAATCATAAAAAAG TGAACTTAATTC-3′
C-terminal FP	5′-**CATATG**TTTATGGAAGAACAAAGATCTTTTAAC-3′
C-terminal RP (MYPE9110 RP)	5′-**GGATCC**TTACTTAATATGATTTTCATTAAG-3′
Glu to Ala MYPE9110 FP	5′-CTAATAAATTTGCATGGTTCACAACTAAAAAAATTAGTAGTAAC-3′
Glu to Ala MYPE9110 RP	5′-GTTACTACTATTTTTTTAGTTGTGAACCATGCAAATTTATTAG-3′
Glu to Asp MYPE9110 FP	5′-GCATTTAGTGATTATGGTCAAAAATTTACTAATAAATTTGACTGG TTCACAAC-3′
Glu to Asp MYPE9110 RP	5′-GTTGTGAACCAGTCAAATTTATTAGTAAATTTTTGACCATAATCACTAAATGC-3′

[a] In the given primer sequences, GAA (Glu)-to-GCA (Ala) or -GAC (Asp) changes are underlined, and the introduced restriction endonuclease sites are in boldface type.

ADP-ribosylation assays. The ADPRT activity of rMYPE9110 and its derivatives was determined as described previously for *M. pneumoniae* CARDS toxin, with slight modifications (17). HeLa cells were grown to 80% confluence, washed, harvested, and sonicated in 50 mM Tris (pH 7.4). HeLa cell lysates were incubated with rMYPE9110 (2.5 μM) in a 50-μl reaction mixture volume of 1 mM GTPγS (Cytoskeleton), 10 mM thymidine (Sigma), 10 mM dithiothreitol (Sigma), 2.5 mM $MgCl_2$ (Sigma), 50 mM Tris (pH 7.4), and 0.2 μM [^{32}P]NAD (800 Ci/mmol; Perkin-Elmer). Fifty-microliter reaction mixture volumes were incubated at 30°C for 1 h, trichloroacetic acid (Sigma) precipitated, and spun at 16,000 × *g* for 10 min. Cell pellets were dissolved in NuPAGE sample buffer (Invitrogen), heated at 70°C for 10 min, and run on NuPAGE 4 to 12% Bis-Tris gradient gels (Invitrogen) for 60 min at 200 V. Gels were transferred onto 0.2-μm nitrocellulose membranes (Protran BA83; Schleicher & Schuell) for 1 h at 15 V and Ponceau (Sigma) stained to determine efficient protein transfer. Membranes were exposed to autoradiographic films (Kodak) from 1 day to 1 week at −80°C and then developed. Similarly, ADP-ribosylation assays were carried out with unlabeled NAD (Sigma) and ADP-ribose (Sigma) as described above. Pertussis holotoxin was purchased from List Biologicals Laboratories, Inc.

NAD-glycohydrolase assay. NAD-glycohydrolase assays were performed according to a modified protocol described previously by Moss et al. (23). Reaction mixture volumes containing 50 mM potassium phosphate (pH 7.4), 4 μM rMYPE9110, 10 mM dithiothreitol (Sigma), 2.5 mM $MgCl_2$ (Sigma), 1 mM GTPγS (Cytoskeleton), and 0.1 mM [carbonyl-^{14}C]NAD (0.05 μCi; Amersham Biosciences) were incubated at 30°C for 1 h. Duplicate samples (100 μl) were applied onto 1-ml columns of Dowex AG-1-X2 (Bio-Rad). Free [carbonyl-^{14}C]nicotinamide was collected with 6 ml of 20 mM Tris (pH 7.4), and radioactivity was quantified (Beckman LS 6500 liquid scintillation counter). *Clostridium botulinum* C3 exoenzyme (List Biologicals Laboratories, Inc.) was used as a positive control for the NAD-glycohydrolase experiments.

Vacuolization conditions. Monolayers of HeLa (ATCC CCL-2) cells were grown to 60 to 70% confluence in 25-cm^2 flasks in MEM (ATCC) supplemented with 10% FBS (Atlas Biologicals) at 37°C and 5% CO_2. Depleted culture medium was replaced by fresh MEM without serum and rMYPE9110 or heat-inactivated rMYPE9110, ranging from 400 ng ml^{-1} to 10 μg ml^{-1}. Heat-inactivated rMYPE9110 and 50 mM Tris (pH 7.4) served as negative controls. After 3 h at 37°C, HeLa cells were incubated in the presence or absence of 10% FBS and 5 mM ammonium chloride (Sigma) and analyzed for vacuolization up to 72 h.

Generation of mouse and rabbit anti-MYPE9110 polyclonal antibodies. Mouse antibodies were generated by immunizing BALB/c mice ($n = 5$), which had been prescreened by immunoblotting to establish the absence of preexisting cross-reactive antibodies to MYPE9110. Mice that showed no reactivity were then injected with a mixture of rMYPE9110 (30 μg) and complete Freund's adjuvant intraperitoneally, boosted with rMYPE9110 (10 μg) and incomplete Freund's adjuvant intraperitoneally, and screened again by Western blot analysis against rMYPE9110 or *M. penetrans* whole-cell lysates. Similarly, anti-rMYPE9110 rabbit antibodies were generated against rMYPE9110 by Strategic Biosolutions, and sera were screened by Western blot analysis against rMYPE9110 and *M. penetrans* whole-cell lysates.

Determination of cell binding by fluorescence-activated cell sorter (FACS) analysis. HeLa cells were grown to confluence in T75 flasks (Corning), trypsinized, and resuspended in PBS. Cells were counted using a hemocytometer, aliquoted (1 × 10^6 cells/tube), and incubated with equimolar concentrations (250 nM) of full-length rMYPE9110, rN-MYPE9110$^{1\text{-}300}$, or PBS–3% FBS (control) for 30 min at 4°C. Cells were washed and incubated with His_6 monoclonal antibody (1:500) (Clontech) in PBS–3% FBS for 30 min at 4°C. Cells were again washed and counterstained with Alexa Fluor 488 goat anti-mouse immunoglobulin G antibody (Invitrogen) in PBS–3% FBS for 30 min at 4°C. Cells were then washed and resuspended in PBS–3% FBS before analysis. Flow cytometry was performed by the Core Flow Cytometry Facility at the University of Texas Health Science Center at San Antonio by using a FACSCalibur system with Cellquest analysis software (Becton-Dickinson and Co., San Jose, CA). Cells were analyzed using forward-scatter and side-scatter gates to include all individual cells stained with Alexa Fluor 488.

Immunofluorescence microscopy analysis. HeLa cells were seeded at 1 × 10^6 cells/well in 24-well plates (Corning) on glass coverslips (1.5 μm; Fisher Scientific) 24 h before intoxication and grown at 37°C in 5% CO_2. Cells were intoxicated with equimolar concentrations (250 nM) of full-length rMYPE9110 or rN-MYPE9110$^{1\text{-}300}$ or without protein in the presence or absence of ammonium chloride and incubated for both 30-min and 1-h postintoxication intervals at 37°C in 5% CO_2. Cells were washed in PBS, fixed in 2% paraformaldehyde (methanol free in PBS) (Electron Microscopy Sciences), and washed three times in PBS. Cells were permeabilized in 0.2% Triton X-100 (Thermo Scientific) in PBS and washed in PBS–1% normal goat serum (NGS). Cells were then incubated with His antibody (1:500) for 1 h in PBS–0.2% NGS, washed, and incubated with goat anti-mouse Alexa Fluor 633 antibody (Invitrogen) in PBS–0.2% NGS for 1 h. Cells were then washed in PBS, incubated with Alexa Fluor 488 phalloidin (Invitrogen) at a dilution of 1:500 for 1 h, washed in PBS, and mounted with Vectashield-1500 with DAPI (4′,6′-diamidino-2-phenylindole). Coverglass slips were sealed with clear nail polish to prevent drying and movement under the microscope. All samples were examined using a multichannel acquisition system operated by AXIO Vision, version 4.7.2, using a Carl-Zeiss Z.1 cell observer. Acquired *z* sections (0.5 μm) were processed using AXIO Vision deconvolution software.

Immune response to *M. penetrans* LAMP and rMYPE9110. Sera were collected from patients attending sexually transmitted disease clinics throughout San Antonio, TX (34), and were evaluated for *M. penetrans* antibodies by Western blot analysis against the lipid-associated membrane proteins (LAMPs) of *M. penetrans*. To obtain LAMP extracts, *M. penetrans* cells were grown to the mid-exponential phase (16 h) and centrifuged, and membrane-associated proteins were enriched by Triton X-114 fractionation as described previously by Riethman et al. (29). Proteins were trichloroacetic acid precipitated from the detergent phase, separated by gel electrophoresis on 4 to 12% NuPAGE gels, and transferred onto nitrocellulose membranes. Protein concentrations were determined by bicinchoninic acid quantitation (Pierce). Serum samples obtained from patients infected with *M. genitalium* that did not react with the LAMP extract of *M. penetrans* served as negative controls. All serum samples were assessed by immunoblotting against total *M. penetrans* proteins (400 ng/strip) and rMYPE9110 (1 μg/strip). Human sera were diluted at 1:100 in 3% milk in Tris-buffered saline–Tween 20 (TBST), while rabbit sera generated against *M. penetrans* whole-cell lysate and rMYPE9110 were diluted at 1:5,000 in 3% milk in TBST. Secondary goat anti-human (Zymed) and goat anti-rabbit (Zymed) sera were diluted in TBST at 1:2,000 and 1:3,000 dilutions, respectively.

RESULTS

Primary sequence and conserved amino acids of *M. penetrans* MYPE9110 suggest ADPRT activity. The identification of the ADP-ribosylating CARDS toxin in *M. pneumoniae* initiated an investigation into other mycoplasma genomes for the presence of a similar ADPRT. BLAST (http://www.ncbi.nlm.nih.gov/BLAST/) (35) analysis revealed both CARDS toxin

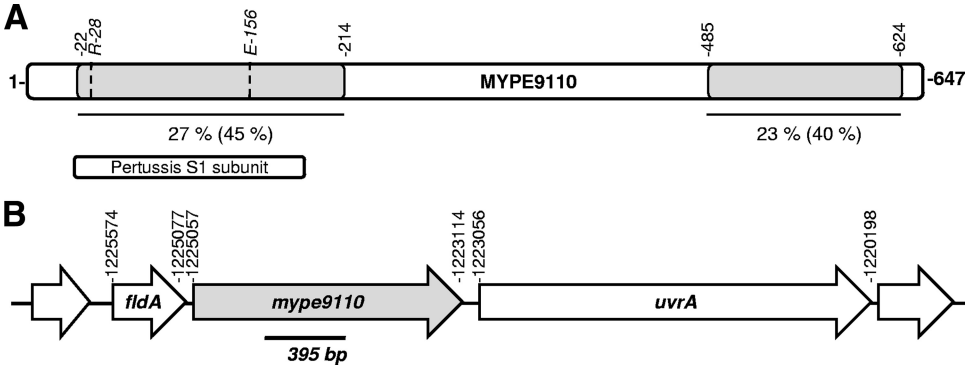

FIG. 1. Schematic representation of MYPE9110 homology with CARDS toxin and genomic organization of MYPE9110. (A) MYPE9110 is an orthologous protein of CARDS toxin. The amino (residues 22 to 214) and carboxyl (residues 485 to 624) amino acid residues that share homology with CARDS toxin are indicated in gray. The percentages of identity and similarity with CARDS toxin (within parentheses) are shown. The amino-terminal region that retains the pertussis S1-like ADPRT domain is indicated. The positions of the essential amino acids necessary for ADPRT are indicated by dotted vertical lines (R28 and E156). (B) The MYPE9110 gene is flanked upstream by *fldA* (flavodoxin) by 19 nucleotides and downstream by *uvrA* (excinuclease ABC subunit A) by 57 nucleotides. The internal 395-bp region used to analyze the transcription of the MYPE9110 gene is shown with bold lines.

and pertussis toxin S1 subunit-like domains within a hypothetical protein of *M. penetrans* annotated MYPE9110 (Fig. 1A). The MYPE9110 gene contains 1,944 nucleotides and is located at positions 1223114 to 1225057 in the genome, flanked by flavodoxin- and excinuclease-encoding genes (Fig. 1B). MYPE9110 has an open reading frame of 647 amino acids, an isoelectric point of 9.2, and a theoretical molecular mass of 78,000 Da. It is predicted to have at least one transmembrane region (amino acids 530 to 541), according to the Dense Alignment Surface transmembrane prediction server (9). The amino-terminal region of MYPE9110 exhibits 27% identity (amino acids 22 to 214) and 45% similarity to *M. pneumoniae* CARDS toxin (Fig. 1A). Members of the bacterial ADPRTs demonstrate limited consensus amino acid sequence conservation, yet they maintain key amino acid residues that are required for enzymatic activity (12). Within the N-terminal region, MYPE9110 retains the conserved arginine (position 28) and glutamate (position 156) residues that are essential for ADPRT activity (Fig. 1A) (4–6). However, unlike CARDS toxin, MYPE9110 does not possess the Ser-Thr-Ser (STS) motif involved in NAD binding (12). The carboxyl region of MYPE9110 shares 23% identity (amino acids 485 to 624) and 40% similarity with the CARDS toxin carboxyl region (Fig. 1A).

Transcriptional analysis of MYPE9110 in GTU-54. To study the expression of MYPE9110, we analyzed the transcription of MYPE9110 during *M. penetrans* GTU-54 growth. As shown in Fig. 2, transcripts of MYPE9110 were detected by RT-PCR using RNA isolated from early-log to stationary phases of growth (3 to 30 h, respectively). As *M. penetrans* enters late-exponential and stationary stages (24 to 30 h), we consistently observed a marked reduction of MYPE9110 transcript levels, suggesting that MYPE9110 is preferentially transcribed during mid-exponential growth (12 to 18 h). The transcription of the constitutive gene *tufA*, which maintained similar levels of transcript through most growth phases, was used for comparative purposes (Fig. 2). RNA, in the absence of reverse transcriptase, served as an internal control at all time points. Similar transcriptional patterns of MYPE9110 were observed for two other clinical strains of *M. penetrans* that were isolated in Texas and France (data not shown) (18).

Site-directed mutagenesis, expression, and purification of rMYPE9110. In order to obtain sufficient amounts of MYPE9110 to ascertain ADPRT activity, rMYPE9110 was expressed in *E. coli* cells. Since mycoplasmas use UGA to encode tryptophan, overlap extension PCR was used to change the seven UGA codons in MYPE9110 to UGG. Thus, we substituted adenines located at nucleotide positions 30, 741, 1473, 1479, 1716, 1761, and 1860 with guanines (Fig. 3A) to encode tryptophan in *E. coli* with primers listed in Table 1. rMYPE9110 was expressed and purified by nickel affinity column chromatography. The recombinant protein migrates as a single 78-kDa band on 10% SDS-polyacrylamide gels, and its sequence was confirmed by matrix-assisted laser desorption ionization–time of flight analysis as described in Materials and Methods (Fig. 3B, lanes 2 and 3).

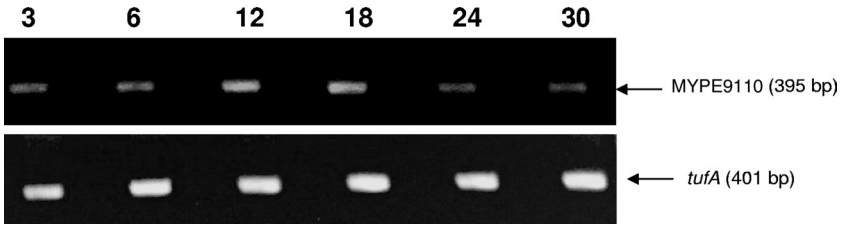

FIG. 2. Transcriptional analysis of the MYPE9110 gene. *M. penetrans* cells were grown in SP-4 medium, and RNA was isolated at 3, 6, 12, 18, 24, and 30 h of growth. RT-PCR ($n = 30$ cycles) was used to confirm MYPE9110 and *tufA* mRNA syntheses in *M. penetrans* GTU-54, and the corresponding cDNA was amplified and resolved by 1% agarose gel electrophoresis.

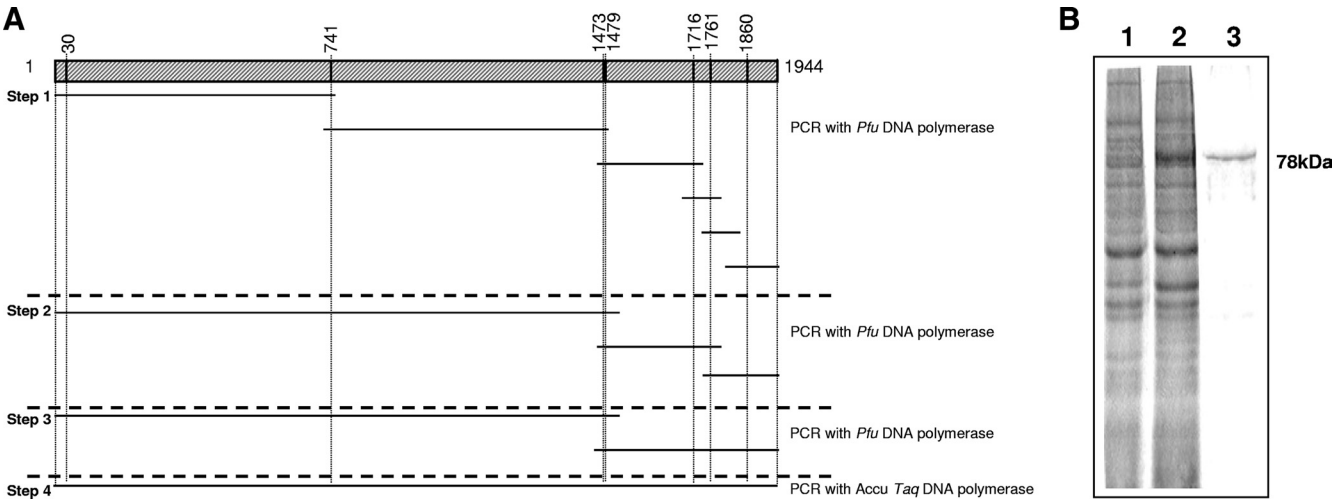

FIG. 3. Cloning, expression, and purification of rMYPE9110. (A) Schematic representation of seven TGA codons corrected to TGG codons. Six overlapping fragments were amplified with the mutagenic primers listed in Table 1 and annealed in order to change UGA-encoding tryptophans to UGG-encoding tryptophans and generate a full-length MYPE9110 gene product to express in *E. coli* cells. (B) Expression and purification of rMYPE9110. rMYPE9110 was expressed and purified in the *E. coli* BL21(DE3) *lpxM* strain, resolved by 10% Laemmli SDS-polyacrylamide gel electrophoresis, and stained with Coomassie brilliant blue R250. Lane 1, uninduced total cell lysate; lane 2, induced total cell lysate; lane 3, purified rMYPE9110.

However, on 4 to 12% gradient NuPAGE gels, which were used for all ADP-ribosylation assays and serological analyses, rMYPE9110 runs just above 64 kDa. In order to further characterize the ADP-ribosylating activity of MYPE9110, an alanine mutant of glutamate-156 (an amino acid essential for the ADP-ribosylating activity of these toxins) was generated. However, this mutant protein showed low-level expression and poor solubility upon purification. We further substituted glutamate-156 with aspartate in order to obtain alternative soluble mutant MYPE9110. Unfortunately, this also yielded similar results of low-level expression and poor solubility, suggesting that a modification of the active site substantially influences protein yield and solubility in *E. coli*.

MYPE9110 exhibits ADPRT activity. To determine whether MYPE9110 possesses ADPRT activity and modifies eukaryotic proteins, we compared ADP-ribosylation patterns between host cells incubated with [^{32}P]NAD in the presence or absence of rMYPE9110. As revealed by autoradiography, we observed intrinsic host cell ADP-ribosylation activity in HeLa cells (Fig. 4, lane 1). However, in the presence of rMYPE9110, we detected additional ^{32}P-labeled HeLa cell proteins of about 23, 25, and 60 kDa (Fig. 4, lane 2). In addition, we observed a broad, intense band above 64 kDa that was strongly ADP-ribosylated (Fig. 4, lane 2). As rMYPE9110 runs near this size on 4 to 12% gradient gels, we further investigated this observation by incubating rMYPE9110 in the presence of [^{32}P]NAD without host cell target proteins and noted auto-ADPRT activity (Fig. 4, lane 3). This was in stark contrast to CARDS toxin of *M. pneumoniae*, where auto-ADP-ribosylation was not detected under similar conditions. Since the N-terminal region of MYPE9110 shares homology to the pertussis toxin S1 subunit and retains essential amino acids for ADPRT activity (Fig. 1A), we analyzed the activity of rN-MYPE9110$^{1\text{-}300}$ and found that it was capable of ADP-ribosylating host proteins, comparable to full-length MYPE9110 (data not shown). This observation indicates that the N terminus is similar to the catalytic A domain of the classical A-B toxins. Interestingly, in contrast to full-length MYPE9110, rN-MYPE9110$^{1\text{-}300}$ (35 kDa) did not undergo auto-ADP-ribosylation, suggesting that the C-terminal region of the protein is the most probable target site for auto-ADP-ribosylation mediated by the N terminus (Fig. 4, lane 4).

To verify that auto-ADP-ribosylation was catalyzed by an enzymatic modification of ADP-ribose, the reaction was performed in the presence of 5 mM unlabeled ADP-ribose (22). Auto-ADP-ribosylation of rMYPE9110 was not affected, consistent with the conclusion that the transfer of ADP-ribose from NAD onto rMYPE9110 is due to enzymatic activity (data not shown).

MYPE9110 exhibits NAD-glycohydrolase activity. In addition to the transferase activity displayed by all bacterial ADPRTs, most of these enzymes have been shown to exhibit NAD-glycohydrolase activity by hydrolyzing NAD to ADP-ribose and nicotinamide, with water acting as the ADP-ribose acceptor. In the presence of nicotinamide-labeled [^{14}C]NAD alone, rMYPE9110 was able to hydrolyze NAD with the release of free ^{14}C-labeled nicotinamide (mean specific activity ± standard deviation of 39 ± 8.4 nmol nicotinamide released h^{-1}). In addition, CARDS toxin exhibited NAD-glycohydrolase activity (specific activity of 48 ± 9.1 nmol nicotinamide released h^{-1}). Under the same experimental conditions, *C. botulinum* exoenzyme C3 (16) served as a positive control (specific activity of 146 ± 4.2 nmol nicotinamide released h^{-1}). NAD-glycohydrolase activities of rMYPE9110 and recombinant CARDS toxin were determined by incubating each ADPRT with [^{14}C]NAD radiolabeled on the nicotinamide moiety in the presence of 50 mM potassium phosphate (pH 7.5) for 1 h at 30°C. Released nicotinamide was quantified by liquid scintillation counting. *C. botulinum* C3 was used as a positive control. The value of the buffer control (no protein added) was subtracted from each data point. Specific activity units are nmoles of released nicotinamide. All assays were run in duplicate.

MYPE9110 exhibits ammonium chloride-dependent vacuolization of mammalian cells. As CARDS toxin of *M. pneu-*

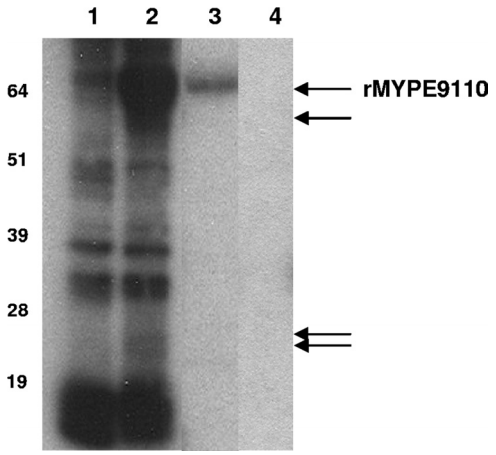

FIG. 4. ADPRT activity of rMYPE9110. HeLa cell lysates were incubated with and without rMYPE9110 in the presence of [^{32}P]NAD, and proteins were separated on a 4 to 12% NuPAGE gel. The gel was transferred onto a nitrocellulose membrane and exposed to X-ray film. Lane 1, HeLa cell lysate and [^{32}P]NAD; lane 2, HeLa cell lysate, [^{32}P]NAD, and rMYPE9110; lane 3, rMYPE9110 and [^{32}P]NAD; lane 4, rN-MYPE9110$^{1-300}$ and [^{32}P]NAD. Arrows indicate radiolabeled host cell proteins and auto-ADP-ribosylated rMYPE9110. Molecular mass markers are indicated on the left in kDa.

moniae caused extensive vacuolization in mammalian cells (17), we examined whether rMYPE9110 demonstrated a similar effect. HeLa cells did not exhibit visible cytopathology in the presence of rMYPE9110 under the same experimental conditions in which *M. pneumoniae* CARDS toxin elicits vacuolization. However, in the presence of ammonium chloride, HeLa cells exposed to exogenous rMYPE9110 displayed distinct vacuolization and cell rounding with a disruption of monolayer integrity, like *Helicobacter pylori* VacA (8). Cytopathology was slow to develop at lower concentrations of rMYPE9110 (400 ng/ml), requiring 48 to 60 h, whereas higher concentrations of rMYPE9110 (5 to 10 μg/ml) elicited the vacuolization of HeLa cells as early as 12 h postintoxication, with widespread vacuolization by 72 h postintoxication (Fig. 5B). The vacuolization of HeLa cells was abolished by the heat inactivation of rMYPE9110 in the presence of ammonium chloride, demonstrating the requirement of an enzymatically active protein in order to elicit the observed vacuolating activity (Fig. 5C). Tris buffer alone, in the presence of ammonium chloride, served as a negative control (Fig. 5A).

Regions of MYPE9110 involved in binding to host cells. Since MYPE9110 was able to cause vacuolization in HeLa cells, we analyzed the binding properties of both full-length MYPE9110 and rN-MYPE9110$^{1-300}$ with HeLa cells by FACS analysis and immunofluorescence. As shown by FACS analysis (Fig. 6A), full-length MYPE9110 was able to bind to HeLa cells at a much higher efficiency (90% of total cells), in contrast to rN-MYPE9110$^{1-300}$, which bound at a markedly reduced level (24% of total cells). As shown in Fig. 6A, HeLa cells intoxicated with full-length rMYPE9110 exhibited a varied distribution of fluorescent toxin, ranging from low to high relative fluorescence intensities. The degree of toxin binding can vary considerably in a given target cell population and could be attributed to the differential expression of receptors in the asynchronous cell population. Similar profiles were previously observed for the binding of *M. penetrans* to human lung cells (2). Correspondingly, as observed by immunofluorescence microscopy (Fig. 6B and C), full-length MYPE9110, irrespective of the presence or absence of ammonium chloride, was able to bind and internalize into the cytoplasm of HeLa cells, in contrast to rN-MYPE9110$^{1-300}$. These events reinforce data from FACS analyses and clearly indicate that the deletion of the C-terminal region of MYPE9110 significantly diminishes the binding of rN-MYPE9110$^{1-300}$ to mammalian cells, consistent with the role of the carboxyl terminus as the receptor-mediating B domain of the A-B family of bacterial toxins. Furthermore, we demonstrate that the binding and internalization of MYPE9110 are not mediated by ammonium chloride.

DISCUSSION

The aim of this study was to characterize the activity of MYPE9110, an annotated hypothetical protein from *M. penetrans* that exhibited amino acid similarities to *M. pneumoniae* CARDS toxin and the pertussis toxin S1 subunit (Fig. 1A). Although members of the ADPRTs share little conservation in primary amino acid sequence, they maintain key spatially conserved amino acid residues that are essential for catalytic activity. Based on these specific amino acid residues that have been experimentally shown to be essential for ADP-ribosylating activity, ADPRTs have been broadly classified into two groups, the cholera toxin (CT) and DT families (12, 24). Mem-

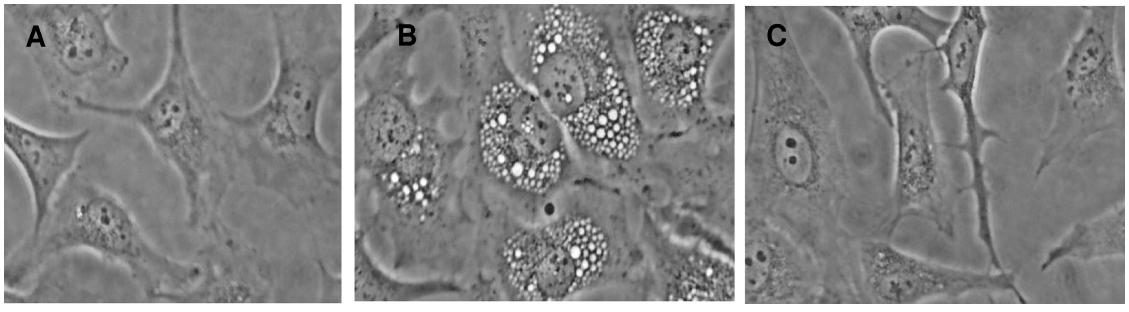

FIG. 5. Cytopathic effects of rMYPE9110 on HeLa cell morphology. HeLa cells were grown in the presence of 50 mM Tris (pH 7.4) and 5 mM ammonium chloride (A), 6 μg ml^{-1} rMYPE9110 and 5 mM ammonium chloride (B), and 6 μg ml^{-1} heat-inactivated rMYPE9110 and 5 mM ammonium chloride (C). All images were captured from HeLa cell cultures grown for 72 h at 37°C.

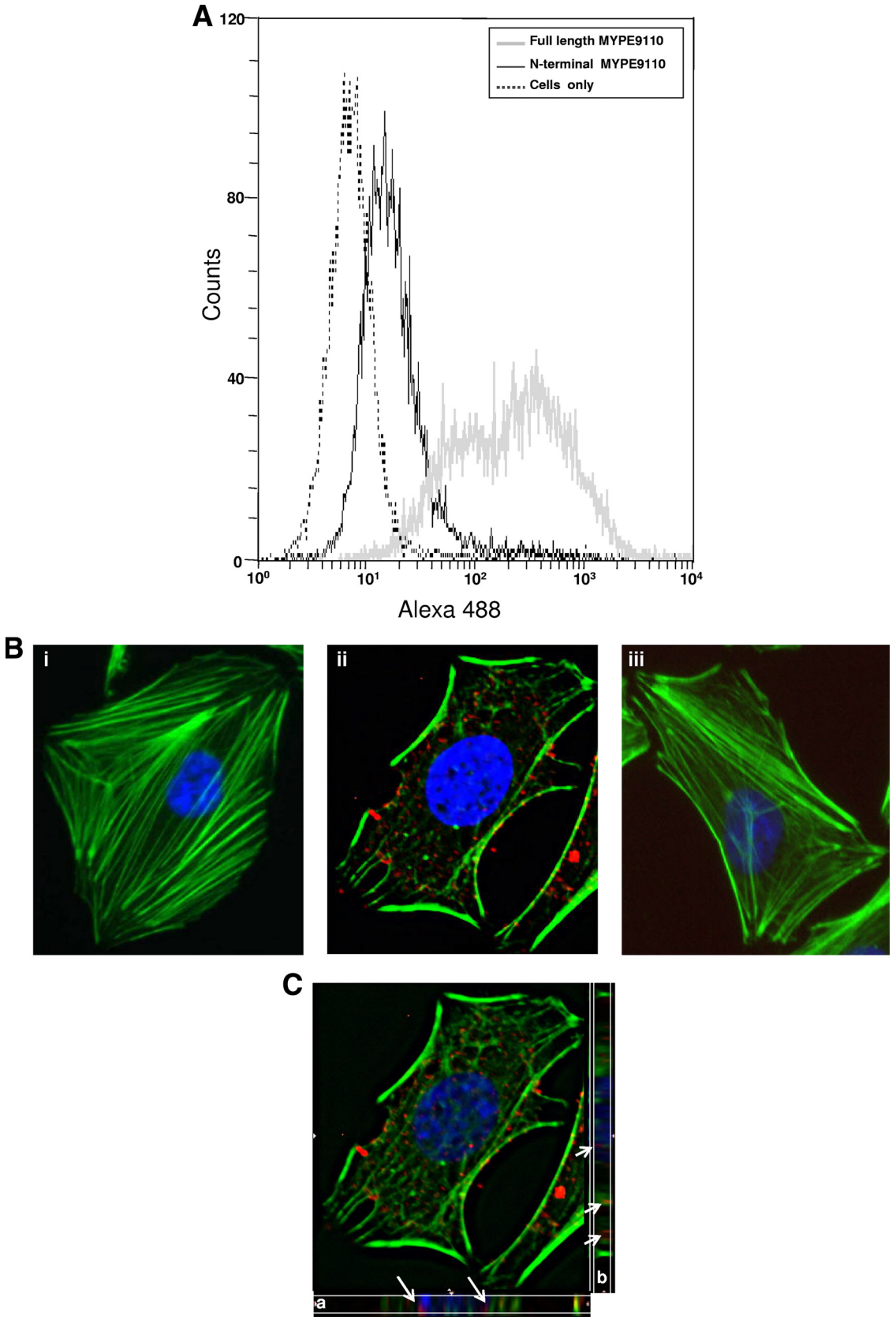

FIG. 6. Properties of binding of rMYPE9110 and rN-MYPE9110$^{1-300}$ to mammalian cells. (A) Binding of full-length rMYPE9110 and rN-MYPE9110$^{1-300}$ determined by FACS analysis. Full-length rMYPE9110 and rN-MYPE9110$^{1-300}$ (both 250 nM) were incubated with 1×10^6 HeLa cells for 30 min, followed by the addition of His antibody (1:500 dilution) and Alexa Fluor 488 (1:500 dilution). The representative histogram

bers of the DT family of ADPRTs contain spatially conserved histidine and tyrosine residues and a catalytic glutamate, whereas CT family members retain a spatially conserved arginine and STS motif and a catalytic glutamate residue. Like the CT family, MYPE9110 possesses the essential arginine and glutamate amino acid residues and exhibits ADP-ribosylating activity even in the absence of the STS motif (Fig. 4). ADPRTs without this STS motif, but still retaining the arginine and glutamate residues, have been classified into the CT family by in silico analysis (24).

The synthesis of the MYPE9110 gene in *M. penetrans* peaks during the mid-exponential phase of growth (Fig. 2), and similar expression patterns were previously observed for other ADP-ribosylating toxins, including the *Bacillus* and *Clostridium* actin-ADP-ribosylating toxins and the *B. pertussis* pertussis toxin (26, 27). Although a growth-dependent transcription of the MYPE9110 gene was observed (Fig. 2), antibodies raised against the recombinant protein did not detect MYPE9110 from *M. penetrans* lysates by Western blot analysis. Like *M. pneumoniae* CARDS toxin, MYPE9110 does not contain a canonical signal sequence, and correspondingly, analysis of SP-4-grown *M. penetrans* culture supernatants did not reveal the presence of MYPE9110 (our unpublished data). These observations were perplexing and suggested that this protein either was expressed in small amounts or required specific conditions for protein stability in vitro. However, sexually transmitted disease patients who showed strong immune responsiveness to *M. penetrans*-specific lipoproteins demonstrated weak to strong immune responses to rMYPE9110, in contrast to uninfected controls, suggesting that MYPE9110 is expressed and immunogenic in vivo (our unpublished data). Whether the expression of MYPE9110 is controlled at the protein level by unique regulatory elements such as a two-component signal transduction system, is released upon contact with host cells, or is introduced during host cell invasion by *M. penetrans* needs further clarification.

Differences between the two mycoplasma toxins *M. penetrans* MYPE9110 and *M. pneumoniae* CARDS toxin were particularly interesting. Even though MYPE9110 shares homology with CARDS toxin, it differs from CARDS toxin in its ADPRT activities (17). Also, a consistent, strong auto-ADP-ribosylation activity was observed with MYPE9110 under all conditions examined, in contrast to CARDS toxin. Auto-ADP-ribosylation was previously documented for other ADPRTs, including *Pseudomonas aeruginosa* ExoS, which uses its C-terminal ADPRT domain to regulate its amino-terminal Rho GTPase-activating activity (28). Similarly, the auto-ADP-ribosylation of MYPE9110 at the C terminus could also regulate fundamental physiological functions.

As mentioned previously, MYPE9110 and CARDS toxin target different host proteins, as evidenced by the unique patterns observed in ADP-ribosylation assays (17). It was previously reported that the conserved polar glutamine/glutamate (Q/E) residue located two amino acids upstream of the catalytic glutamate in ADPRTs may determine substrate specificity (15). The substitution of this glutamate with the polar lysine residue in MYPE9110 may account for distinctions between CARDS toxin and MYPE9110, as alterations of targets have been linked to changes in this amino acid in eukaryotic ADPRTs (30). Both of these mycoplasma toxins were able to hydrolyze NAD in the absence of target proteins, although the *Clostridium* C3 and *M. pneumoniae* CARDS toxins exhibited higher levels of activity, which could be due to the absence of the STS motif in MYPE9110. Amino acid changes within this NAD-binding region have been shown to affect the strength of NAD binding between the CT and DT family members (12).

Bacterial ADPRTs can target low-molecular-weight GTP-binding proteins and affect a range of cellular functions, from signaling and translocation of proteins to altering cellular shape and movement (11). As *M. penetrans* triggers the aggregation of cytoskeletal proteins in mammalian cells (13) and as we have observed MYPE9110-mediated ADP-ribosylation of low-molecular-weight proteins, we cannot rule out the possibility of small G proteins as targets of MYPE9110 ADP-ribosylation (Fig. 4). Whether the ADPRT activity of MYPE9110 is involved in membrane ruffling or cytoskeletal rearrangements requires further clarification. An excellent experimental approach to identify the role of MYPE9110 is to generate a null mutant of MYPE9110 in *M. penetrans*. However, in contrast to several other mycoplasmas, genetic manipulation of *M. penetrans* has not been achieved.

Like CARDS toxin, MYPE9110 also exhibits a vacuolating activity although under different experimental conditions. As VacA of the gastrointestinal pathogen *H. pylori* requires acid activation as well as ammonium chloride for vacuolization (8), MYPE9110 of the urogenital tract pathogen *M. penetrans* needs weak bases like ammonium chloride for vacuolization, which could change the pH of endosomes and, in turn, favor MYPE9110 activation. This biological behavior of *M. penetrans* suggests specific adaptive mechanisms for tissue tropism and site colonization during infection and persistence. Particularly interesting is that a vacuolating activity was previously ascribed to actively growing *M. penetrans* bacteria in HeLa cell lines, although the basis for vacuole formation was thought to be associated with the formation of oxidative radicals (3a). Our detection of a genome-encoded protein in *M. penetrans* that in vitro exhibits an ADP-ribosylating and vacuolating activity suggests a link between successful parasitism, cytopathology, and this potential bona fide virulence determinant.

presents cell numbers plotted on the *y* axis and log fluorescence intensity plotted on the *x* axis. Cells incubated without protein were used as a control. (B) Comparative binding and internalization activities of full-length rMYPE9110 and rN-MYPE9110$^{1-300}$ determined by immunofluorescence. HeLa cells were incubated with no protein (control) (i) or intoxicated with either full-length rMYPE9110 (ii) or rN-MYPE9110$^{1-300}$ (iii) (250 nM) and analyzed by fluorescence microscopy. Cells were stained with DAPI (nucleus, blue), Alexa Fluor 633 (rMYPE9110, red), and Alexa Fluor 488 (phalloidin, green). All representative HeLa cell images are shown in the absence of ammonium chloride and at a ×400 magnification. (C) Localization of rMYPE9110 within intoxicated HeLa cells. Shown is a representative HeLa cell stained with DAPI (nucleus), Alexa Fluor 633 (rMYPE9110), and Alexa Fluor 488 (phalloidin). Digital orthogonal sections through *z*-series data sets (0.5 μm) confirmed that HeLa cell-associated rMYPE9110 is inside the cell. Images show HeLa cells intoxicated with rMYPE9110 and extended views of the horizontal (a) and vertical (b) *z* projections of HeLa cells. Arrows (white) indicate the localization of rMYPE9110 immunofluorescence in the horizontal and vertical *z* projections.

The recent discovery of the first ADP-ribosylating toxin in mycoplasmas, *M. pneumoniae* CARDS toxin, was an exciting development in the mycoplasma field. Similarly, the detection of a related but distinct ADP-ribosylating toxin in *M. penetrans* lends credence to the role of ADPRTs in mycoplasma-mediated pathogenesis. Further investigation into the role of this unique ADP-ribosylating, vacuolating toxin would help to clarify the biology and pathogenicity of *M. penetrans* and host cell-mycoplasma interplay.

ACKNOWLEDGMENTS

The project described was supported by award U19AI045429 from the National Institute of Allergy and Infectious Diseases and the Kleberg Foundation. Data were generated in the Core Flow Cytometry Facility, which is supported by the University of Texas Health Science Center at San Antonio, NIH-NCI grant P30 CA54174 (Cancer Therapy and Research Center), NIH-NIA grant P30 AG013319 (Nathan Shock Center), and NIH-NIA grant P01AG19316.

We thank Joel Moss for his helpful discussions, Marianna Cagle for raising antibodies against rMYPE9110, Krishnan Manickam for his help with microscope images, and Rose Garza for her assistance with assembling the manuscript.

The content is solely the responsibility of the authors and does not necessarily represent the official views of the National Institute of Allergy and Infectious Diseases or the National Institutes of Health.

REFERENCES

1. **Aktories, K., M. Barmann, I. Ohishi, S. Tsuyama, K. H. Jakobs, and E. Habermann.** 1986. Botulinum C2 toxin ADP-ribosylates actin. Nature **322:** 390–392.
2. **Baseman, J. B., M. Lange, N. L. Criscimagna, J. A. Giron, and C. A. Thomas.** 1995. Interplay between mycoplasmas and host target cells. Microb. Pathog. **19:**105–116.
3. **Bendjennat, M., A. Blanchard, M. Loutfi, L. Montagnier, and E. Bahraoui.** 1997. Purification and characterization of *Mycoplasma penetrans* Ca^{2+}/Mg^{2+}-dependent endonuclease. J. Bacteriol. **179:**2210–2220.

3a. **Borovsky, Z., M. Tarshis, P. Zhang, and S. Rottem.** 1998. Protein kinase C activation and vacuolation in HeLa cells invaded by *Mycoplasma penetrans*. J. Med. Microbiol. **47:**915–922.

4. **Burnette, W. N., W. Cieplak, V. L. Mar, K. T. Kaljot, H. Sato, and J. M. Keith.** 1988. Pertussis toxin S1 mutant with reduced enzyme activity and a conserved protective epitope. Science **242:**72–74.
5. **Carroll, S. F., and R. J. Collier.** 1984. NAD binding site of diphtheria toxin: identification of a residue within the nicotinamide subsite by photochemical modification with NAD. Proc. Natl. Acad. Sci. USA **81:**3307–3311.
6. **Cieplak, W., W. N. Burnette, V. L. Mar, K. T. Kaljot, C. F. Morris, K. K. Chen, H. Sato, and J. M. Keith.** 1988. Identification of a region in the S1 subunit of pertussis toxin that is required for enzymatic activity and that contributes to the formation of a neutralizing antigenic determinant. Proc. Natl. Acad. Sci. USA **85:**4667–4671.
7. **Cognet, I., A. B. de Coignac, G. Magistrelli, P. Jeannin, J. P. Aubry, K. Maisnier-Patin, G. Caron, S. Chevalier, F. Humbert, T. Nguyen, A. Beck, D. Velin, Y. Delneste, M. Malissard, and J. F. Gauchat.** 2003. Expression of recombinant proteins in a lipid A mutant of *Escherichia coli* BL21 with a strongly reduced capacity to induce dendritic cell activation and maturation. J. Immunol. Methods **272:**199–210.
8. **Cover, T. L., S. G. Vaughn, P. Cao, and M. J. Blaser.** 1992. Potentiation of *Helicobacter pylori* vacuolating toxin activity by nicotine and other weak bases. J. Infect. Dis. **166:**1073–1078.
9. **Cserzo, M., E. Wallin, I. Simon, G. von Heijne, and A. Elofsson.** 1997. Prediction of transmembrane alpha-helices in prokaryotic membrane proteins: the dense alignment surface method. Protein Eng. **10:**673–676.
10. **Dallo, S. F., and J. B. Baseman.** 2000. Intracellular DNA replication and long-term survival of pathogenic mycoplasmas. Microb. Pathog. **29:**301–309.
11. **Domenighini, M., M. Pizza, and R. Rappuoli.** 1995. Bacterial ADP-ribosyltransferases, p. 59–80. *In* J. Moss, B. Iglewski, M. Vaughan, and A. Tu (ed.), Bacterial toxins and virulence factors in disease, 1st ed., vol. 8. Marcel Dekker, Inc., New York, NY.
12. **Domenighini, M., and R. Rappuoli.** 1996. Three conserved consensus sequences identify the NAD-binding site of ADP-ribosylating enzymes, expressed by eukaryotes, bacteria and T-even bacteriophages. Mol. Microbiol. **21:**667–674.
13. **Giron, J. A., M. Lange, and J. B. Baseman.** 1996. Adherence, fibronectin binding, and induction of cytoskeleton reorganization in cultured human cells by *Mycoplasma penetrans*. Infect. Immun. **64:**197–208.
14. **Ho, S. N., H. D. Hunt, R. M. Horton, J. K. Pullen, and L. R. Pease.** 1989. Site-directed mutagenesis by overlap extension using the polymerase chain reaction. Gene **77:**51–59.
15. **Holbourn, K. P., C. C. Shone, and K. R. Acharya.** 2006. A family of killer toxins. Exploring the mechanism of ADP-ribosylating toxins. FEBS J. **273:** 4579–4593.
16. **Jung, M., I. Just, J. van Damme, J. Vandekerckhove, and K. Aktories.** 1993. NAD-binding site of the C3-like ADP-ribosyltransferase from *Clostridium limosum*. J. Biol. Chem. **268:**23215–23218.
17. **Kannan, T. R., and J. B. Baseman.** 2006. ADP-ribosylating and vacuolating cytotoxin of *Mycoplasma pneumoniae* represents unique virulence determinant among bacterial pathogens. Proc. Natl. Acad. Sci. USA **103:**6724–6729.
18. **Kannan, T. R., and J. B. Baseman.** 2000. Hemolytic and hemoxidative activities in *Mycoplasma penetrans*. Infect. Immun. **68:**6419–6422.
19. **Kannan, T. R., D. Provenzano, J. R. Wright, and J. B. Baseman.** 2005. Identification and characterization of human surfactant protein A binding protein of *Mycoplasma pneumoniae*. Infect. Immun. **73:**2828–2834.
20. **Lo, S. C., M. M. Hayes, R. Y. Wang, P. F. Pierce, H. Kotani, and J. W. Shih.** 1991. Newly discovered mycoplasma isolated from patients infected with HIV. Lancet **338:**1415–1418.
21. **Locht, C., and J. M. Keith.** 1986. Pertussis toxin gene: nucleotide sequence and genetic organization. Science **232:**1258–1264.
22. **Masignani, V., E. Balducci, F. Di Marcello, S. Savino, D. Serruto, D. Veggi, S. Bambini, M. Scarselli, B. Arico, M. Comanducci, J. Adu-Bobie, M. M. Giuliani, R. Rappuoli, and M. Pizza.** 2003. NarE: a novel ADP-ribosyltransferase from *Neisseria meningitidis*. Mol. Microbiol. **50:**1055–1067.
23. **Moss, J., V. C. Manganiello, and M. Vaughan.** 1976. Hydrolysis of nicotinamide adenine dinucleotide by choleragen and its A protomer: possible role in the activation of adenylate cyclase. Proc. Natl. Acad. Sci. USA **73:**4424–4427.
24. **Pallen, M. J., A. C. Lam, N. J. Loman, and A. McBride.** 2001. An abundance of bacterial ADP-ribosyltransferases—implications for the origin of exotoxins and their human homologues. Trends Microbiol. **9:**302–307.
25. **Pappenheimer, A. M., Jr.** 1977. Diphtheria toxin. Annu. Rev. Biochem. **46:**69–94.
26. **Popoff, M. R., and B. G. Stiles.** 2006. Bacterial toxins and virulence factors targeting the actin cytoskeleton and intercellular junctions, p. 154–181. *In* J. E. Alouf and M. R. Popoff (ed.), The comprehensive sourcebook of bacterial toxins, 3rd ed. Academic Press, London, United Kingdom.
27. **Rambow-Larsen, A. A., and A. A. Weiss.** 2004. Temporal expression of pertussis toxin and Ptl secretion proteins by *Bordetella pertussis*. J. Bacteriol. **186:**43–50.
28. **Riese, M. J., U. M. Goehring, M. E. Ehrmantraut, J. Moss, J. T. Barbieri, K. Aktories, and G. Schmidt.** 2002. Auto-ADP-ribosylation of *Pseudomonas aeruginosa* ExoS. J. Biol. Chem. **277:**12082–12088.
29. **Riethman, H. C., M. J. Boyer, and K. S. Wise.** 1987. Triton X-114 phase fractionation of an integral membrane surface protein mediating monoclonal antibody killing of *Mycoplasma hyorhinis*. Infect. Immun. **55:**1094–1100.
30. **Ritter, H., F. Koch-Nolte, V. E. Marquez, and G. E. Schulz.** 2003. Substrate binding and catalysis of ecto-ADP-ribosyltransferase 2.2 from rat. Biochemistry **42:**10155–10162.
31. **Sasaki, Y., A. Blanchard, H. L. Watson, S. Garcia, A. Dulioust, L. Montagnier, and M. L. Gougeon.** 1995. In vitro influence of *Mycoplasma penetrans* on activation of peripheral T lymphocytes from healthy donors or human immunodeficiency virus-infected individuals. Infect. Immun. **63:**4277–4283.
32. **Sasaki, Y., J. Ishikawa, A. Yamashita, K. Oshima, T. Kenri, K. Furuya, C. Yoshino, A. Horino, T. Shiba, T. Sasaki, and M. Hattori.** 2002. The complete genomic sequence of *Mycoplasma penetrans*, an intracellular bacterial pathogen in humans. Nucleic Acids Res. **30:**5293–5300.
33. **Schering, B., M. Barmann, G. S. Chhatwal, U. Geipel, and K. Aktories.** 1988. ADP-ribosylation of skeletal muscle and non-muscle actin by *Clostridium perfringens* iota toxin. Eur. J. Biochem. **171:**225–229.
34. **Shain, R. N., J. M. Piper, E. R. Newton, S. T. Perdue, R. Ramos, J. D. Champion, and F. A. Guerra.** 1999. A randomized, controlled trial of a behavioral intervention to prevent sexually transmitted disease among minority women. N. Engl. J. Med. **340:**93–100.
35. **Tatusova, T. A., and T. L. Madden.** 1999. BLAST 2 Sequences, a new tool for comparing protein and nucleotide sequences. FEMS Microbiol. Lett. **174:** 247–250.
36. **Wang, R. Y., J. W. Shih, T. Grandinetti, P. F. Pierce, M. M. Hayes, D. J. Wear, H. J. Alter, and S. C. Lo.** 1992. High frequency of antibodies to *Mycoplasma penetrans* in HIV-infected patients. Lancet **340:**1312–1316.
37. **Yanez, A., L. Cedillo, O. Neyrolles, E. Alonso, M. C. Prevost, J. Rojas, H. L. Watson, A. Blanchard, and G. H. Cassell.** 1999. *Mycoplasma penetrans* bacteremia and primary antiphospholipid syndrome. Emerg. Infect. Dis. **5:**164–167.

Editor: S. R. Blanke